A NOVEL LOW SIZE, WEIGHT AND POWER MULTIBAND GNSS ANTENNA

Dr Steven Christie
Arralis Technologies Ltd.

Abstract: In this paper, a novel miniature, surface mountable circularly polarised antenna is proposed for multiband multi-constellation Global Navigation Satellite Systems (GNSS). The antenna is designed to operate over multiple GPS, Galileo and GLONASS bands located over two distinct frequency spans of 1.164 GHz to 1.239 GHz (covering GPS L5, Galileo E5a, GPS L2), and 1.559 GHz to 1.610 GHz (covering GPS L1, Galileo E1, GLONASS G1). A circularly polarised spiral antenna, which is meandered to reduce its surface area, is used to produce RHCP radiation, with a novel high impedance surface providing electrical isolation at the back-side of the antenna, whilst significantly miniaturising the antenna profile compared to existing techniques.

1. Introduction

Due to the proliferation of geo-location technologies, there is a requirement for the development of small, light-weight and low-profile antenna terminals which can be surface mounted, for vehicular or on-body applications. Geo-location systems require Circularly Polarised (CP) antennas to efficiently receive satellite signals, and wide bandwidths are also desirable to provide multiband multi-constellation coverage for built in redundancy. At operating frequencies as low as 1.16 GHz, where the free space wavelength is approximately 258 mm, these combined requirements become a challenging design issue. One antenna which produces wideband CP radiation is the spiral antenna. These radiate bi-directionally with a front-lobe and a back-lobe of equal gain, Figure 1a, and some design modifications are therefore required for surface mounted applications to electrically isolate the back side of the spiral and prevent grounding effects. This can be achieved using a $\lambda/4$ cavity and ground plane to reflect the back lobe such that it adds in phase with the front lobe, Figure 1b, which has been demonstrated to increase the antenna gain by approximately 3 dB [1]. Whilst this method effectively isolates the antenna back-side, it is inherently narrowband (due to $c = f \lambda_0$), and can lead to thick devices (65 mm at 1.16 GHz). Absorber placed behind the antenna can be used to absorb the back lobe radiation over wide bandwidths, which has been demonstrated at thicknesses as small as $\lambda_0/14$ [2], but this method reduces radiation efficiency by approximately 50 %. An alternative method which has been demonstrated in recent years is to place the spiral antenna above a High Impedance Surface (HIS) (also known as an Electromagnetic Bandgap Material (EBG)) [3], [4], [5], [6]. At the frequency of operation, the HIS acts like a Perfect Magnetic Conductor (PMC), and a wave at normal incidence is reflected with 0° phase change. By careful design of the HIS, the reflection phase can be controlled such that the spiral back lobe is reflected in phase with the front lobe with a thickness << $\lambda/4$ (with gaps as low as $\lambda_0/14$ previously demonstrated [6]). By using a HIS, some control over the flatness of the reflection phase can be achieved, for example through choice of the dielectric material, however bandwidths in the order of 32% (as required to cover from GPS L5/Gallileo E5a up to GLONASS G1), are not practically achievable using standard techniques and materials. In this paper, the author presents a novel HIS, which, when used in conjunction with a spiral antenna, can operate over two distinct frequency bands which themselves cover multiple GNSS bands; 1.164 GHz to 1.239 GHz (covering GPS L5, Galileo E5a, GPS L2); and 1.559 GHz to 1.610 GHz (covering GPS L1, Galileo E1, GLONASS G1); at thicknesses as small as $\lambda_0/30$, and with a surface area of 96 mm x 86 mm. Dual band operation has previously been achieved using nested HIS, whereby elements operating at a higher frequency are placed underneath the corresponding high frequency active region at the centre of the spiral, with elements operating at a lower frequency placed around these under the spiral's lower frequency active region. In [7] such a design is presented which operates at 4.8 GHz and 6.5 GHz, and

in [8] a similar approach is used to operate at 3 GHz, 6 GHz and 9 GHz. For the multi-band, multi-constellation application discussed here however, dual band operation is required at frequencies spaced at ratios as small as 1:1.25, and hence a novel split HIS approach is taken.

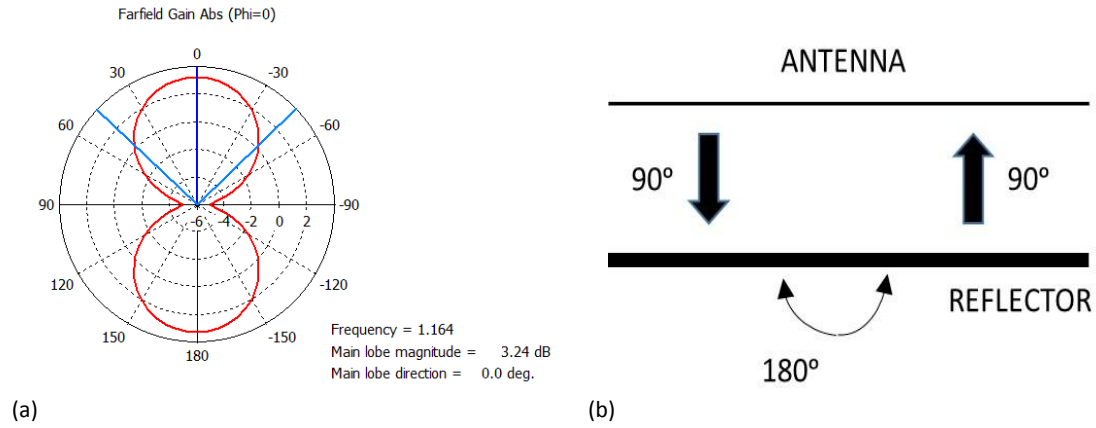

(a) (b)

Figure 1. A typical spiral antenna radiation pattern; (a) front-lobe and back lobe; (b) phasing provided by a λ/4 cavity and reflector

2. Meandered Spiral Design

The radiating section of the antenna is based on an Archimedean spiral antenna, Figure 2a. It consists of two spiral arms, which are excited in antiphase at their inner terminations. When the circumference of the antenna is much smaller than the wavelength, the antenna acts as a twinline, with energy well confined to the slot between them, and any radiation from the two arms cancelling out due to their phasing. Radiation occurs at a frequency f_r, when the path length from point A to point B on the same spiral arm is equal to one half of the guide wavelength, $\lambda_g/2$, which produces an additional electrical phase delay of 180° between the two points. Points A and A' are symmetrically located on opposing arms, and thus, the current at these points is in antiphase. Therefore, at the frequency f_r, the currents at points A' and B are in equi-phase (and likewise at points A and B'), and the spiral partially radiates. The active region of the antenna is therefore a ring of circumference λ_g, or radius $\lambda_g/2\pi$. This condition for radiation is inherently provided over wide bandwidths due to the spiral geometry, with higher frequencies emitted from closer to the centre of the antenna, and the spiral's outer radius determining the lower cut-off frequency. Because the spiral radiates only partially, residual current is reflected from the ends of the arms, which increases the VSWR and interferes with the incident current, increasing the axial ratio. In practice, spiral radii in the order of 1.5 – 2 times $\lambda_g/2\pi$ are typically required in order to reduce this effect, as well as increasing the conductor resistivity or using resistive loading at the outer spiral terminations [9].

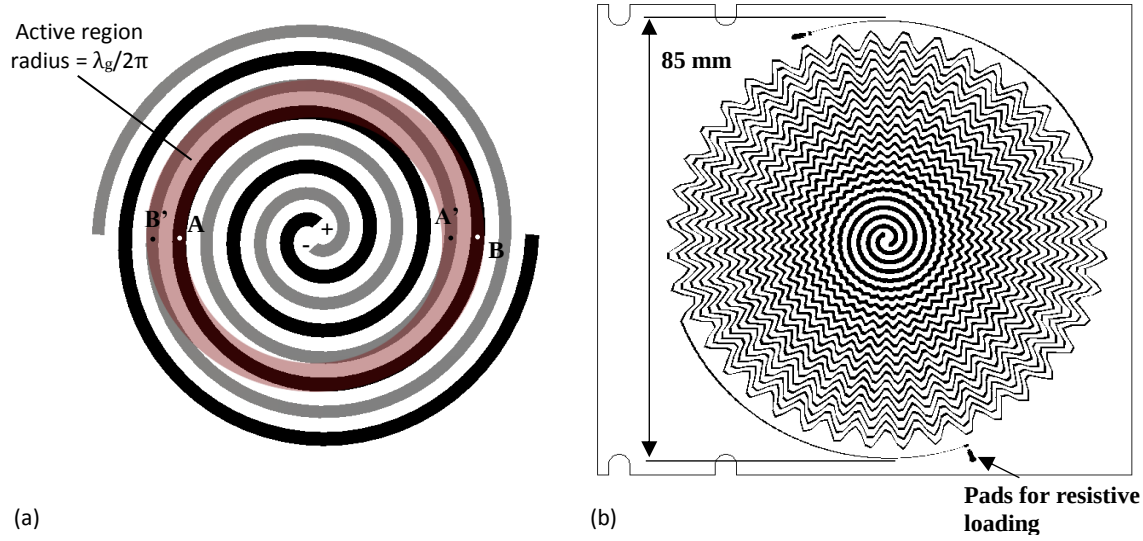

Figure 2. Archimedean spiral antenna; (a) radiating region; (b) meandered spiral antenna design

The Archimedean spiral design is carried out using CST Microwave Studio Time Domain Solver. To reduce its surface area, the spiral is meandered, Figure 2b, and placed on a 0.127 mm thick, high permittivity Rogers RT3010 substrate (ε_r = 10.2, $tan\delta$ = 0.0023), with the spiral geometry described using equation 1 [10]. The spiral tapers from a width of 0.85 mm at the feed, to 0.425 mm at the end of the meandered section, and then to 5 µm at the termination points, which makes the arms more highly resistive to reduce reflections, and provides a widening gap towards the outer extremities to increase radiation efficiency at the lower frequencies. To further reduce reflections, pads are placed at the ends of the spiral arms which are each terminated using 250 Ω loads. A standard spiral design would typically be in the order of 120 – 150 mm diameter to achieve radiation at frequencies as low as 1.164 GHz, but by using a meandered spiral on RT3010 substrate with resistive loading, the diameter is reduced to 85 mm, whilst the antenna has a predicted VSWR < 2:1 and radiates with predicted front and back lobe gains of greater than 3 dB, as shown in Figure 1a.

$$r = r_o + a\emptyset + m \cdot \frac{(\emptyset - \emptyset_{start})}{(\emptyset_{end} - \emptyset_{start})} \cdot \sin n\emptyset \qquad 1$$

where:-
r_o is the original radius of the spiral (0.5mm)
a is the spiral constant (0.541mm/rad)
$\emptyset$ is the rotation angle (rad)
$\emptyset_{start}$ is the starting rotation angle (12.566 rad)
$\emptyset_{end}$ is the ending rotation angle (72.2959 rad)
m is the sine-wave amplitude constant (2)
n is the sine meander frequency constant (40)

3. High Impedance Surface Design

A standard HIS, illustrated in Figure 3a, typically consists of a dielectric sandwiched between a top layer of periodically repeating resonant elements and a continuous metal ground plane. In this case, the HIS resonant elements used are patches, which are grounded using vias. The HIS is separated from the spiral antenna using a 3 mm thick Rohacell foam layer (ε_r = 1.05), and a cross-section of the composite antenna structure is shown in Figure 3b. The design aim is for the HIS to reflect the antenna back lobe such that it arrives at the antenna with 0° reflection phase. This can be only be achieved at a single frequency, and so the design aim is to achieve this 0° response at the centre frequency, with

as flat a reflection phase response as possible. A general design trade-off is that a flatter reflection phase response can be achieved by increasing the thickness and permittivity of the HIS dielectric, however, it is not practical to achieve a flat phase response over 1.164 GHz – 1.610 GHz using a periodic HIS consisting of a single patch size: this would require much thicker and/or higher permittivity dielectrics than are available. Moreover, the use of a nested HIS is not possible because the two bands are too close together in frequency, with the two bands' spiral active regions overlapping partially. Instead, a 3.8 mm thick, high permittivity Rogers RT6010 laminate is used in the HIS to maximise the bandwidth, and the novel approach is taken to split the HIS into two halves, each of which have different patch widths, as illustrated in Figure 4a. On one side are two larger patches with edge widths of w_{p1} and on the other, six smaller patches with widths of w_{p2}. Because the spiral radiates from a ring shaped active region, the HIS region with patch widths w_{p1} reflects the lower frequency band with the desired phasing producing constructive interference, whilst reflecting the higher frequency band with improper phasing, giving destructive interference. Likewise the other half, with path widths w_{p2} cancels radiation in the lower frequency band, whilst reflecting the upper frequency band with good phase characteristics. The novel HIS, which combines the two different patch sizes, therefore effectively gives an average of the two HIS gain responses (weighted slightly towards the response of the 25.1mm patch, which occupies a larger surface area). The HIS and Rohacell layers are modelled as a unit cell in CST Microwave Studio, and the patch dimensions are varied to achieve 0° reflection phase at 1.2 GHz and 1.575 GHz. Using a gap of 4.8 mm between adjacent patches, patch widths of w_{p1} = 34.6 mm provide 0° phase at 1.2 GHz, with ±80° over 1.164 GHz – 1.239 GHz, and w_{p2} = 25.1 mm provide a reflection phase zeroed at 1.575 GHz, with ±40° over the 1.559 GHz – 1.610 GHz span. The reflection phases of the two patches are shown in Figure 4b. The composite antenna, consisting of the spiral above the HIS, with a 3mm Rohacell spacer layer, is modelled in CST, and simulated in the Time Domain Solver with approximately 23 million mesh cells. The antenna achieves predicted boresight RHCP gains of between -0.96 dB to 1.7 dB (with gain > 0 dB over 1.164 – 1.591 GHz), with VSWR < 2:1 across the lower frequency band, and < 2.5:1 across the upper band. The predicted axial ratio is typically less than 4 dB across the operating frequencies: in the lower band, the predicted axial ratio is 5.37 dB at 1.164 GHz, decreasing to 1 dB at 1.239 GHz, and in the upper band it is 0.83 dB at 1.559 GHz, increasing to 4.1 dB at 1.610 GHz. In contrast, at 1.3 GHz, a frequency for which neither HIS patch size provides good reflection phase (see Figure 4b), the VSWR is 4:1, and the axial ratio is 17 dB. The RHCP gains are typically quite low due to the very close proximity of the spiral to the HIS and dielectric, and the use of resistive loading, which both reduce the radiation efficiency, in combination with the axial ratios of > 0 dB, which indicates reduced power radiated in RHCP.

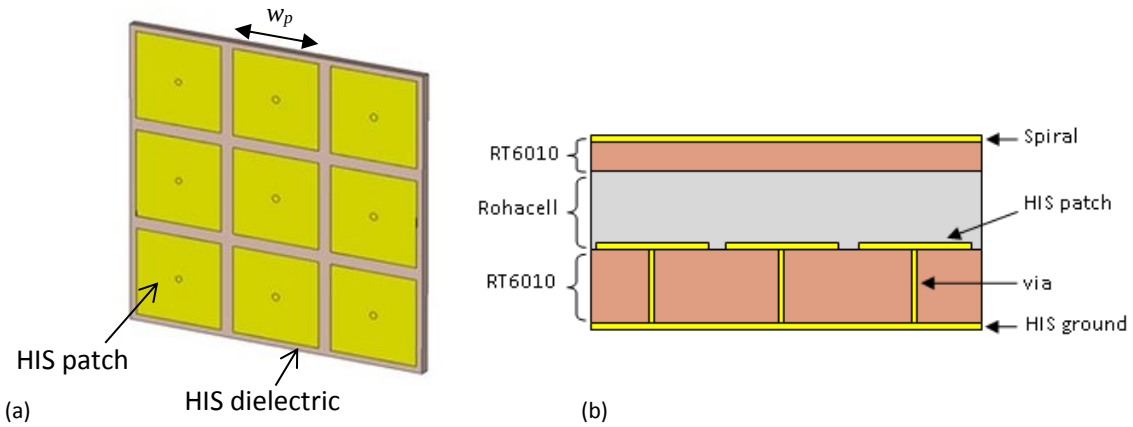

Figure 3. High Impedance Surface; (a) standard topology; (b) cross-section of HIS and spiral antenna structure

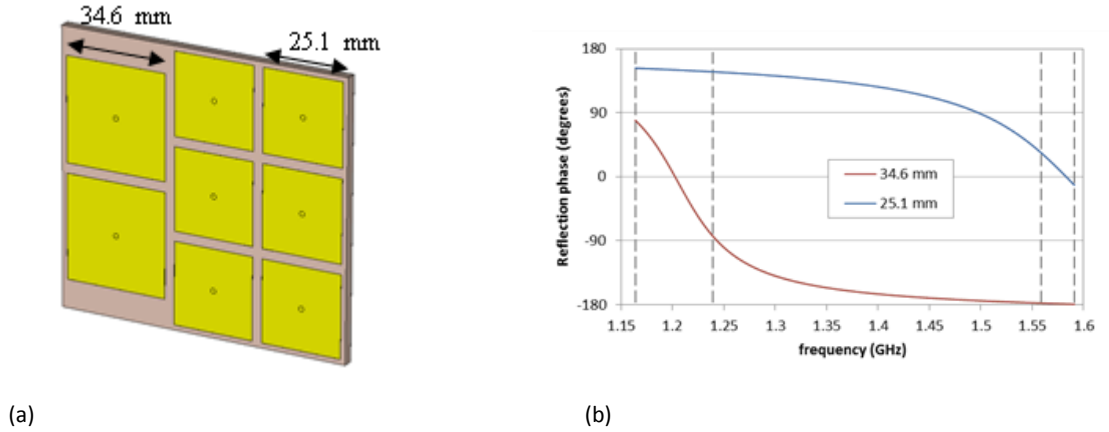

(a) (b)

Figure 4. Novel HIS; (a) Split configuration; (b) reflection phase response of individual square patches with 25.1 mm and 34.6 mm edge widths

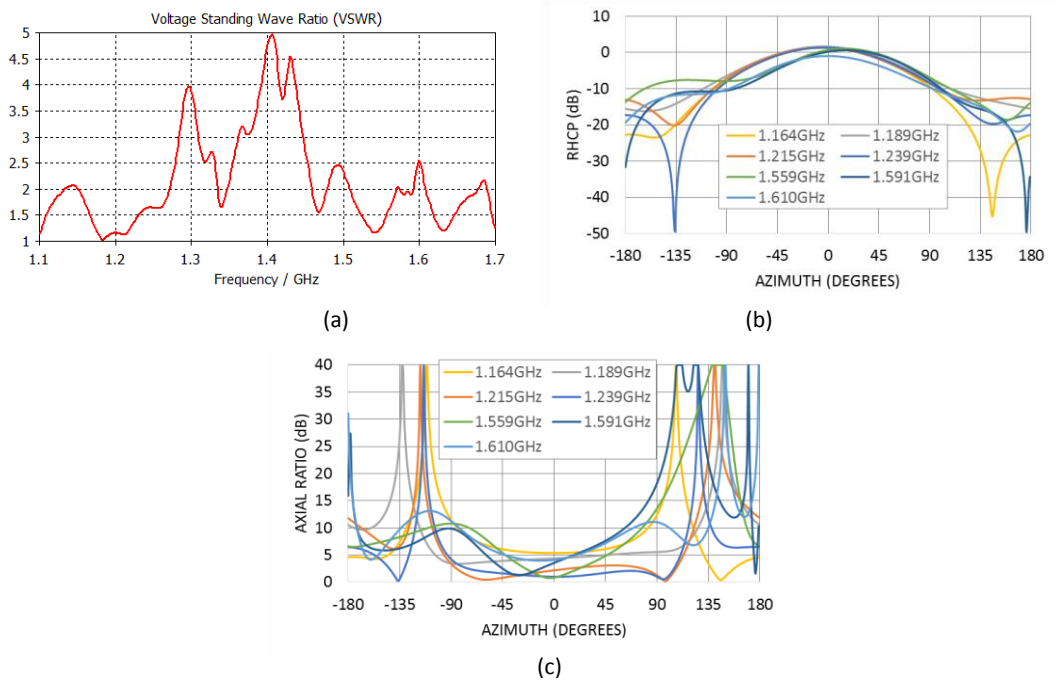

(a) (b)

(c)

Figure 5. Predicted performance of spiral and novel split HIS configuration (w_{p1} = 25.1 mm, w_{p2} = 34.6 mm); (a) VSWR; (b) RHCP gain predictions; (c) Axial ratio

4. Conclusions

A composite antenna is presented which consists of a right-hand circularly polarised Archimedean spiral placed above a novel split HIS. By meandering the spiral, and using high permittivity substrates for the spiral and HIS the thickness is reduced to $\lambda_0/30$, and the diameter of the spiral to 85 mm. The novel split HIS allows the antenna to operate over two closely spaced frequency bands, each of which are made wideband through use of a 3.8 mm thick, high permittivity RT6010 substrate. In this way, the antenna is capable of operating over 1.164 GHz to 1.239 GHz (covering GPS L5, Galileo E5a, GPS L2), and 1.559 GHz to 1.610 GHz (covering GPS L1, Galileo E1, GLONASS G1), whilst providing a typical predicted performance of; VSWR < 2:1; gain > 0 dB; axial ratio <4.5 dB; and occupying a volume of 96 mm x 86 mm x 6.7 mm. For further work, an active antenna design will be fabricated. The antenna's balanced 130 Ω input impedance will be matched to an unbalanced 50 Ω feed using a wideband Marchand balun, and for high gain, an LNA will be integrated into the feed network to provide active gain with a bypass option.

Acknowledgements: This paper is based upon work supported by Innovate UK, under SBRI Competition Number MOD_236, File Reference 971438.

5. References

[1] H. Nakano, K. Nogami, S. Arai, H. Mimaki and J. Yamauchi, "A Spiral Antenna Backed by a Conducting Plane Reflector," *IEEE Transactions on Antennas and Propagation,* vol. 34, no. 6, pp. 791-796, 1986.

[2] H. Nakano, S. Sasaki, H. Oyanagi and J. Yamauchi, "Cavity-backed Archimedean spiral antenna with strip absorber," *IET Microwaves, Antennas and Propagation,* vol. 2, no. 7, pp. 725-730, 2008.

[3] T. H. Liu, W. X. Zhang, M. Zhang and K. F. Tsang, "Low Profile Spiral Antenna with PBG Substrate," *Electronics Letters,* vol. 36, no. 9, pp. 779-780, 2000.

[4] D. Sievenpiper, L. Zhang, R. F. Jiminez Broas, N. G. Alexopolous and E. Yablonovitch, "High-Impedance Electromagnetic Surfaces with a Forbidden Frequency Band," *IEEE Transactions on Microwave Theory and Techniques,* vol. 47, no. 11, pp. 2059-2074, 1999.

[5] J. M. Bell and M. F. Iskander, "A Low-Profile Archimedean Spiral Antenna Using an EBG Ground Plane," *IEEE Antennas and Wireless Propagation Letters,* vol. 3, pp. 223-226, 2004.

[6] H. Nakano, K. Kikkawa, N. Kondo, Y. Iitsuka and J. Yamauchi, "Low-Profile Equiangular Spiral Antenna Backed by an EBG Reflector," *IEEE Transactions on Antennas and Propagation,* vol. 57, no. 5, pp. 1309-1318, 2009.

[7] H. Nakano, H. Oyanagi and J. Yamauchi, "Spiral Antenna Above a Composite HIS Reflector," in *APSURSI*, 2010.

[8] S. Mohamad, R. Cahill and V. Fusco, "Selective High Impedance Surface Active Region Loading of Archimedean Spiral Antenna," *IEEE Antennas and Wireless Propagation Letters,* vol. 13, pp. 810-813, 2014.

[9] T. E. Morgan, "18 - 40 GHz Spiral Antenna," in *17th European Microwave Conference*, 1987.

[10] Y.-W. Wang, G.-M. Wang and H.-Y. Zeng, "Design of a New Meander Archimedean Spiral Antenna," *Microwave and Optical Technology Letters,* vol. 52, no. 10, pp. 2384-2387, 2010.